Vision Research 49 (2009) 2891–2901

Contents lists available at ScienceDirect

Vision Research

journal homepage: www.elsevier.com/locate/visres

Low- and high-level motion perception deficits in anisometropic and strabismic amblyopia: Evidence from fMRI

Cindy S. Ho *, Deborah E. Giaschi

Department of Ophthalmology and Visual Sciences, University of British Columbia, Children's and Women's Health Centre of British Columbia, Canada

ARTICLE INFO

Article history:
Received 6 November 2007
Received in revised form 21 July 2009

Keywords:
Amblyopia
Dmax
Feature matching
fMRI
Motion

ABSTRACT

Maximum motion displacement (Dmax) is the largest dot displacement in a random-dot kinematogram (RDK) at which direction of motion can be correctly discriminated [Braddick, O. (1974). A short-range process in apparent motion. *Vision Research, 14*, 519–527]. For first-order RDKs, Dmax gets larger as dot size increases and/or dot density decreases. It has been suggested that this increase in Dmax reflects greater involvement of high-level feature-matching motion mechanisms and less dependence on low-level motion detectors [Sato, T. (1998). Dmax: Relations to low- and high-level motion processes. In T. Watanabe (Ed.), *High-level motion processing, computational, neurobiological, and psychophysical perspectives* (pp. 115–151). Boston: MIT Press]. Recent psychophysical findings [Ho, C. S., & Giaschi, D. E. (2006). Deficient maximum motion displacement in amblyopia. *Vision Research, 46*, 4595–4603; Ho, C. S., & Giaschi, D. E. (2007). Stereopsis-dependent deficits in maximum motion displacement. *Vision Research, 47*, 2778–2785] suggest that this "switch" from low-level to high-level motion processing is also observed in children with anisometropic and strabismic amblyopia as RDK dot size is increased and/or dot density is decreased. However, both high- and low-level Dmax were reduced relative to controls. In this study, we used functional MRI to determine the motion-sensitive areas that may account for the reduced Dmax in amblyopia In the control group, low-level RDKs elicited stronger responses in low-level (posterior occipital) areas and high-level RDKs elicited a greater response in high-level (extra-striate occipital–parietal) areas when activation for high-level RDKs was compared to that for low-level RDKs. Participants with anisometropic amblyopia showed the same pattern of cortical activation although extent of activation differences was less than in controls. For those with strabismic amblyopia, there was almost no difference in the cortical activity for low-level and high-level RDKs, and activation was reduced relative to the other groups. Differences in the extent of cortical activation may be related to amblyogenic subtype.

1. Introduction

Clinically, amblyopia is characterized by reduced visual acuity in one eye despite normal ocular health and optimal refractive correction. In unilateral amblyopia, the fellow (unaffected) eye demonstrates normal visual acuity. In addition to visual deprivation, amblyopia may be caused by strabismus, anisometropia or a combination of both strabismus and anisometropia.

Psychophysical tests showing visual losses other than reduced visual acuity implicate deficits in both P/ventral (form) and M/dorsal (motion) pathways (Milner & Goodale, 1995; Ungerleider & Mishkin, 1982). In addition to reduced visual acuity, there are well-documented deficits in other aspects of spatial vision such as low-contrast acuity, contrast sensitivity, positional acuity and spatial localization (for reviews see Asper, Crewther, & Crewther, 2000; Levi, 1991). There have also been reports of deficits in temporal and motion processing (Schor & Levi, 1980a; Schor & Levi, 1980b; Steinman, Levi, & McKee, 1988). Evidence for impairment of motion mechanisms in amblyopia has grown and includes reported deficits involving oscillatory movement displacement (Buckingham, Watkins, Bansal, & Bamford, 1991; Kelly & Buckingham, 1998), motion-defined form (Giaschi, Regan, Kraft, & Hong, 1992; Ho et al., 2005), motion after-effect (Hess, Demanins, & Bex, 1997), maximum motion displacement (Ho & Giaschi, 2006; Ho & Giaschi, 2007; Ho et al., 2005), and global motion (Ellemberg, Lewis, Maurer, Brar, & Brent, 2002; Simmers, Ledgeway, Hess, & McGraw, 2003). There have been numerous reports of abnormal motion perception in both the amblyopic and the fellow eye suggesting that these deficits are not well accounted for by reduced visual acuity (or other form perception deficits) in amblyopic eyes (Giaschi et al., 1992; Ho & Giaschi, 2006; Ho & Giaschi, 2007; Ho et al., 2005; Simmers et al., 2003).

* Corresponding author. Address: Department of Ophthalmology and Visual Sciences, University of British Columbia, Room A146, BC's Children's Hospital, 4480 Oak Street Vancouver, BC, Canada V6H 3V4. Fax: +1 604 875 2683.
E-mail address: cindyh@interchange.ubc.ca (C.S. Ho).

0042-6989/$ - see front matter © 2009 Elsevier Ltd. All rights reserved.
doi:10.1016/j.visres.2009.07.012

Our recent studies in amblyopia have focused on deficits of maximum motion displacement (Dmax). Dmax is the largest displacement at which the direction of a random-dot kinematogram (RDK) can be reliably discriminated (Braddick, 1974). If the displacement is small and all dots are shifted in the same direction (100% coherence), direction discrimination is not difficult because the motion perceived is smooth and continuous. As the displacement approaches the maximum displacement value (Dmax), direction discrimination of the apparent motion is still possible but more difficult because the motion appears to be less coherent. The value of Dmax may be restricted by the receptive field size of low spatial-frequency-tuned motion detectors at a low-level of motion processing and/or by the efficiency of spatial feature-matching at high levels of motion processing (Nishida & Sato, 1995; Sato, 1998; Snowden & Braddick, 1990).[1] It has been suggested that as dot probability is decreased or dot size is increased, motion processing involves low-level mechanisms to a lesser extent and is biased more toward high-level motion mechanisms (Sato, 1998; Smith & Ledgeway, 2001). There have been reports of amblyopic deficits in Dmax for both low-level and high-level RDKs (Ho & Giaschi, 2006; Ho & Giaschi, 2007). Our findings confirm that this mechanism "switch" is intact in amblyopia but it is associated with an overall decrease in Dmax.

Several other studies of amblyopia suggest that high-level motion processing is more impaired than low-level motion processing. The M pathway in the human visual system projects dorsally and includes high-level, motion-sensitive extra-striate areas: V3A (Tootell et al., 1997), V5/MT+ (Tootell et al., 1995; Zeki et al., 1991) and regions of the posterior parietal cortex (PPC) (Cheng, Fujita, Kanno, Miura, & Tanaka, 1995; Dupont, Orban, De Bruyn, Verbruggen, & Mortelmans, 1994; Orban et al., 2006; Sunaert, Van Hecke, Marchal, & Orban, 1999). Simmers and colleagues reported deficits in MT using first- and second-order global motion stimuli (Simmers, Ledgeway, & Hess, 2005; Simmers et al., 2003) as well as deficits in MSTd using translational, rotational, and radial optic flow patterns (Simmers, Ledgeway, Mansouri, Hutchinson, & Hess, 2006) in an amblyopic population. We have previously reported deficits in high-level attentive tracking (Ho & Giaschi, 2006). Attentive tracking (Cavanagh, 1992) is a high-level motion task that involves feature-matching mechanisms. The results of these studies implicate extra-striate motion-sensitive areas as part of the neural deficit underlying amblyopia. The attentive-tracking deficits seen in amblyopia (Ho et al., 2006) are likely associated with impairment of PPC (to which the dorsal visual pathway projects) because Culham and colleagues identified parietal activation using similar attentive-tracking tasks with functional MRI (Culham et al., 1998). Furthermore, PPC is implicated in high-level motion perception because patients with parietal lesions show deficits in motion perception for high- but not low-level tasks (Battelli et al., 2001).

Although several studies of amblyopia have demonstrated psychophysical deficits consistent with abnormal high-level motion mechanisms, there has been limited direct neuroimaging evidence to date associating extra-striate motion-sensitive brain areas with these behavioral deficits in amblyopic participants. The aim of this study was to investigate the extent to which the high-level (and likely the feature-based) motion system (and PPC) is impaired in amblyopia. The RDK stimulus parameters were kept consistent with those from our earlier studies (Ho & Giaschi, 2006; Ho & Giaschi, 2007). We assessed children with strabismic and anisometropic amblyopia and controls on two luminance-defined, high-level motion conditions (decreased dot density and increased dot size) as well as a low-level baseline (small dots, densely spaced) condition. Given our hypothesis that abnormal neural activity in extra-striate cortex may explain the reported behavioral Dmax deficits, less involvement of dorsal extra-striate areas in amblyopic participants relative to control participants during a direction discrimination task with high-level RDKs (compared to the low-level baseline RDK) was expected.

2. Methods

2.1. Participants

2.1.1. Control group

Four control children were tested, ranging in age from 14 to 16 years (M = 15.4 yrs, SD = 0.9 yrs). All of the subjects tested were visually mature as Dmax has been shown to reach adult levels between age 7 and 8 years (Parrish, Giaschi, Boden, & Dougherty, 2005). All children included had distance and near monocular line visual acuity (VA) equivalent to or better than 6/6 or 0.4 M, respectively (Jose & Atcherson, 1977). Both acuity cut-off values represent letter size with detail of 1 min when measured at 6 m and 40 cm, respectively. Distance line VA was measured using the Regan 96% contrast letter chart and near VA was measured using the University of Waterloo near vision test card. Stereoacuity, assessed using the Randot Stereotest (Stereo Optical Co., Inc.), was required to be equivalent to or better than 40″. Worth-4-Dot (W4D) testing (reviewed in Rutstein & Daum, 1998, chap. 5) was used to test for fusion and scored to give another measure of binocularity. The scoring was as follows:

5 = constant fusion
4 = intermittent fusion with intermittent diplopia
3 = constant diplopia
2 = intermittent suppression
1 = constant suppression.

All control subjects, when tested in the dark, were required to have a score of 5 when tested at 1 m. No control subject had a history of ocular pathology or abnormal visual development.

2.1.2. Amblyopic group

The subjects were referred from the Department of Ophthalmology at the Children's and Women's Health Centre of British Columbia, and from other local clinics. The ages and clinical details of the amblyopic children are summarized in Table 1. Data were collected from three amblyopic children with strabismus (M = 14.4 yrs, SD = 1.0 yrs) and four with anisometropia (M = 14.2

[1] Feature-matching is a characteristic of the long-range (but not the short-range) motion system proposed by Braddick (1974). Since Braddick's short-range and long-range classification, several other theories of motion perception have evolved. For example, Cavanagh and Mather (1990) suggest that low-level mechanisms process first-order stimuli (luminance- or color-defined) and that high-level mechanisms process second-order motion stimuli (motion- and stereo-defined). Lu and Sperling (reviewed in 2001) propose three separate motion systems: a first-order system responding to luminance-defined stimuli, a second-order system responding to contrast- or motion-defined stimuli, and a third-order system which is based on the "salience map" of a moving stimulus. Nishida and Sato (1995) propose a model in which low-level and high-level mechanisms are based on spatial-frequency-tuned motion detectors and feature matching mechanisms, respectively (see also Sato, 1998). The mechanism that dominates is largely dependent on the stimulus parameters chosen (see also Smith & Ledgeway, 2001; Snowden & Braddick, 1990). Decreasing dot density and/or increasing dot size of first-order, luminance-defined RDKs create a bias towards high-level motion mechanisms. Nishida & Sato's model is most appropriate for this study given that all motion stimuli used are first-order. Because all stimuli are luminance-defined, this fMRI study differs from those looking at the neural substrates underlying first-order and second-order motion (see for example: Claeys, Lindsey, De Schutter, & Orban, 2003; Dumoulin, Baker, Hess, & Evans, 2003; Dupont, Sary, Peuskens, & Orban, 2003; Nishida, Sasaki, Murakami, Watanabe, & Tootell, 2003; Seiffert, Somers, Dale, & Tootell, 2003; Smith, Greenlee, Singh, Kraemer, & Hennig, 1998) which may not necessarily involve similar high-level mechanisms to those we are studying.

Table 1
Clinical Details for Amblyopic Participants.

	Age (years)	Decimal VA (amblyopic)	Decimal VA (fellow)	Stereoacuity (sec of arc)	Worth-4-Dot	Refraction	Clinical details & ocular deviation
S + A	13.5	0.43	1.26	500	1	OD: plano OS:+3.25	Diagnosed age 10; no patching or surgery; 8Δ LXT
S	14.1	1.09	1.22	500	3	OD: plano OS: plano	Surgery age 9 months; no patching; 6Δ RET
S	15.5	1.09	1.26	70	3	OD: plano OS: plano	Diagnosed age 3; patching; no surgery; 15Δ LXT
A	12.9	0.89	1.15	50	4	OD:+4.00 + 2.50 × 85 OS:+3.75 + 4.00 × 11	Diagnosed age 3; patching; 4Δ esophoria
A	14.1	0.73	1.03	20	5	OD: −1.50 OS: plano	Diagnosed age 5; patching; orthophoria
A	14.1	0.55	1.19	40	5	OD:+6.00 + 0.50 × 90 OS:+5.50	Diagnosed age 2; patching; 2Δ esophoria
A	15.7	0.71	1.00	20	5	OD:+0.25 + 0.50 × 63 OS: −2.00	Diagnosed age 3; patching; 8Δ exophoria

S: strabismus; A: anisometropia; RET: right esotropia; LXT: left exotropia; OD: right eye; OS: left eye; Δ: prism dioptre.

yrs, *SD* = 1.1 yrs). To be included in the amblyopic group, there had to be greater than a 1 line difference in VA between the amblyopic and fellow eye in the presence of anisometropia and/or strabismus. For those with a 1 line difference in visual acuity, there had to be a history of occlusion therapy. To be classified as anisometropic in this study, there had to be at least a 1.00 dioptre difference in the spherical equivalent refractive error between amblyopic and fellow eyes. None of the subjects included had eccentric fixation, latent or manifest nystagmus, anomalous retinal correspondence, or oculomotor dysfunction with the exception of strabismus. To avoid the possibility of testing subjects with bilateral amblyopia, the inclusion criteria for the fellow eye were the same as those for the control subjects, described above.

Although one of the three strabismic children also had anisometropia, they were included in the strabismic subgroup. Psychophysically classifying aniso-strabismic individuals into "strabismic amblyopia" is not uncommon (e.g. Barnes, Hess, Dumoulin, Achtman, & Pike, 2001; Demanins, Wang, & Hess, 1999; Mansouri, Allen, & Hess, 2005; Mussap & Levi, 1999). Children with strabismus demonstrate different spatial deficits than children with pure anisometropia even if the strabismus is early onset and/or coexists with anisometropia (Birch & Swanson, 2000). In this study, children with stereoacuity <500 s were considered binocular and those with no measurable stereoacuity (>500 s) on the Randot Stereotest were considered non-binocular. In general, the anisometropic and strabismic groups represented binocular and non-binocular groups, respectively. The average stereoacuity and Worth-4-Dot scores for the anisometropic group in this study were 33 s (*SD* = 15) and 4.8 (*SD* = 0.5). The same scores in the strabismic group were 357 s (*SD* = 248) and 2.3 (*SD* = 1.2).

2.2. Psychophysics

Prior to the fMRI sessions, individual Dmax values for direction discrimination were determined in the psychophysics laboratory. This was done to equate the difficulty level of the behavioral task in the scanner and to account for the expected variability in Dmax across subjects.

2.2.1. Stimulus

The psychophysical tasks were programmed in Matlab and run on a Macintosh Power G4 laptop computer. The stimuli were displayed on a 17″ monitor with a resolution of 800 × 600 (horizontal × vertical) pixels and a refresh rate of 60 Hz. Subject responses were collected with a Gravis Gamepad Pro.

The visual stimuli for all conditions of the Dmax task consisted of randomly generated patterns of white dots (100 cd/m^2) on a black background (5 cd/m^2). The viewing distance was 70 cm. The entire random-dot display subtended a visual angle of 25.4 × 19.2 deg (horizontal × vertical).

Each subject performed the task under three display parameters in each eye: 20 min dot size at 5% dot density (Condition 1), 20 min dot size at 0.5% dot density (Condition 2), and 1 deg dot size at 5% dot density (Condition 3). The dot sizes listed above represent the diameter of each round dot in the display. Each RDK consisted of 10 frames and the duration of each frame presentation was 200 ms (12 screen refreshes at 60 Hz). No inter-stimulus interval was used. A total of six threshold values were recorded for each subject.

2.2.2. Procedure

The study was approved by the University of British Columbia's Behavioural Research Ethics Board. All thresholds were determined in one session that lasted approximately 30 min. For the fMRI phase of the study, the eyes were dissociated by using red–green filters (Bernell Vision Training Products Inc., Mishawaka, IN, USA) to allow for monocular testing (see Section 2.3.1). Use of clinical red–green filters is a standard method for binocular dissociation used in orthoptic evaluation and training. To be consistent, the psychophysical thresholds were determined while the subjects wore the same MRI-compatible glasses with the red–green filters in place such that the right eye viewed through a red filter and the left eye through a green filter. The luminance of the projected stimulus through red and green filters was measured with a photometer. Neutral density filters were added until the luminance of the projected stimuli was equal. To make the red filtered stimulus equiluminant to the green filtered stimulus, a 0.3 neutral density filter was placed over the red filter for all psychophysical and fMRI stimulus presentations. Prescribed optical correction was worn under red–green filters throughout testing for subjects requiring refractive correction. The non-tested eye was occluded. Testing was performed under diffuse illumination with lights directed away from the display screen to prevent glare. Subject responses were self-paced and subjects were asked to guess the correct response if they were unsure. Feedback was provided for the subjects throughout the trials. The eye tested first was randomly varied for each subject.

For each trial, the random-dot display was displaced by a given jump size, upward or downward, at 100% coherence, for 10 consecutive frames of animation. The task was direction discrimination of the apparent motion. A two-alternative forced-choice (2AFC) paradigm was used, in which the probability of accurately guessing the correct response was 50%.

As the displacement increased, the task of direction discrimination became more difficult. All conditions began with a jump size of 0.3 deg that all participants could perform easily with 100% accuracy. Jump size was adjusted such that it increased after two correct responses, and decreased after one incorrect response. Jump size was halved, beginning at the 4th reversal, for each incorrect response. The staircase ended after the 15th reversal in jump size or after 60 trial presentations, whichever occurred first. Throughout testing, subjects were asked to maintain fixation on a cross in the middle of the screen. The displacement levels were chosen based on previous findings (Ho & Giaschi, 2006; Ho &

Giaschi, 2007). To ensure that the task was understood before each session, the participants were asked to do a practice staircase.

2.2.3. Threshold calculations

Psychometric functions were fitted using the Psignifit toolbox version 2.5.41 for Matlab (see http://bootstrap-software.org/psignifit/) which implements the maximum-likelihood method described by Wichmann and Hill (2001). Threshold (Dmax) was defined using the stimulus level at which performance was 75% correct, halfway between the guess rate (50% correct) and perfect performance (100% correct) for a 2AFC paradigm. The six thresholds were recorded to be used later in the fMRI scans below.

Table 2 lists the psychophysical thresholds obtained. As expected, Condition 2 and 3 (the high-level conditions) gave larger Dmax values than Condition 1 (the baseline low-level condition) in both amblyopic and control groups. Performance did not differ across the groups.

2.3. Functional MRI

To minimize head motion, we limited the scan length to less than an hour for each session because of the younger age of some of the participants. Every child participated in a simulator session prior to scanning to ensure that they would be comfortable in the scanner on test day, and to screen for children who might have difficulty remaining still. During this simulator session, each subject was also run through the experimental paradigms to ensure familiarity with the tasks and procedures. Just prior to the actual scans, the head was supported and padded with foam within the head coil by the MRI technologists to minimize the likelihood of head movements. Subjects were also discouraged from speaking during the length of the scan.

2.3.1. Data acquisition

A Philips Gyroscan Intera 3 Tesla MRI scanner with a phased array head coil (SENSE) was used to acquire fMRI data. During a session, echo-planar imaging (EPI) was used to collect functional data in four $T2^*$-weighted scans (TE = 30 ms, TR = 2000 ms, FOV = 240 mm, 3 mm isotropic voxel size, 80 × 80 mm matrix [reconstructed: 128 × 128 mm matrix, 1.88 × 1.88 × 3 mm voxel size]). Whole-brain volumes were collected in 36 interleaved axial slices (3 mm thick, 1 mm inter-slice gap). At the end of each scanning session a high-resolution anatomic whole brain image was collected with a T1-weighted scan (FOV: 256 mm, matrix: 256 × 256, voxel size: 1 × 1 × 1 mm).

Equiluminant red and green filters were placed in an MRI-compatible frame with the red filter always in front of the right eye. For those requiring refractive correction, either contact lenses or prescription MRI-compatible lenses were worn under the red–green glasses. Red and green filters, cut from the same filters used in the glasses, were placed over the projector, and changed throughout the scan, to allow for monocular testing. The eye tested first was randomly varied by changing the order in which the red and green filters were placed over the projector.

The visual stimuli were back projected with an LCD projector onto a screen, 53 cm behind the participant's head, and viewed through a mirror that was 15 cm from the participant's eyes. Subject responses were obtained using a fiber optic response system (Lumitouch).

2.3.2. Visual stimuli & experimental design

The RDKs used for the psychophysics were modified into two different block design fMRI runs that were viewed with each eye. The runs were composed of white dots on a black background with a central white fixation cross (display width: 25.3 deg; height: 19.4 deg). The dots moved either upwards or downwards with 100% coherence. Fig. 1 illustrates the fMRI paradigm used in each of the runs.

Each of the two Dmax runs had six 14 s epochs that were repeated for four cycles. The psychophysical Dmax values for both eyes of each participant were used to determine the jump sizes in each epoch. A total of six thresholds were needed per subject (3 RDK conditions × 2 eyes). The epochs were designed to compare cortical activation for: (1) random motion, easy coherent motion (dot displacement at ½ Dmax), and difficult coherent motion (dot displacement at Dmax) direction discrimination; and (2) the baseline low-level RDK (Condition 1); and the two high-level RDK conditions (Condtions 2 or 3), i.e. to compare the RDK stimuli within each of the types of motion. We were interested in determining the pattern of cortical activation for low-level and high-level (increased dot size; reduced dot density) RDKs with dot displacement specifically set at Dmax but also wanted to know whether this cortical activation pattern would be altered for sub-threshold stimuli (i.e. decreasing task difficulty by using displacement at ½ Dmax).

The six epoch parameters [dot display; dot displacement; motion coherence] for the first Dmax run are listed below:

(1) 20 min dots at 5% density (Condition 1); Dmax or ½ Dmax (randomized); 0%.
(2) 20 min dots at 5% density (Condition 1); ½ Dmax; 100%.
(3) 20 min dots at 5% density (Condition 1); Dmax; 100%.
(4) 20 min dots at 0.5% density (Condition 2); Dmax or ½ Dmax (randomized); 0%.
(5) 20 min dots at 0.5% density (Condition 2); ½ Dmax; 100%.

Table 2
Individual Dmax values (degrees of visual angle) for low-level (Condition 1) and high-level (Conditions 2 & 3) RDKs.

Group	Subject	Condition 1: *baseline* (20 min dots at 5% density)	Condition 2: *decr. dot density* (20 min dots at 0.5% density)	Condition 3: *incr. dot size* (1 deg dots at 5% density)
S	A	AE: 2.25; FE: 1.26	AE: 4.32; FE: 4.31	AE: 4.25; FE: 4.50
	B	AE: 3.41; FE: 2.46	AE: 4.56; FE: 5.00	AE: 5.31; FE: 5.90
	C	AE: 1.30; FE: 1.32	AE: 3.29; FE: 3.20	AE: 5.25; FE: 4.50
A	D	AE: 1.74; FE: 2.00	AE: 3.75; FE: 4.30	AE: 4.94; FE: 4.00
	E	AE: 2.25; FE: 3.26	AE: 4.37; FE 4.39	AE: 3.41; FE: 3.98
	F	AE: 2.00; FE: 3.31	AE: 4.00; FE: 3.41	AE: 5.50; FE:5.00
	G	AE: 1.04; FE: 0.93	AE: 3.20; FE: 4.36	AE: 3.25; FE: 3.26
	Mean (SD)	*AE: 2.00 (0.77); FE: 2.10 (0.97)*	*AE: 3.93 (0.54); FE: 4.14 (0.62)*	*AE: 4.56 (0.93); FE: 4.45 (0.84)*
C	H	RE: 3.00; LE: 2.75	RE: 3.32; LE: 4.00	RE: 4.25; LE: 4.25
	I	RE: 2.33; LE: 2.77	RE: 4.31; LE: 5.22	RE: 5.17; LE: 6.00
	J	RE: 1.53; LE: 2.00	RE: 3.07; LE 3.50	RE: 6.36; LE: 4.32
	K	RE: 1.25; LE: 1.51	RE: 3.80; LE: 4.00	RE: 2.38; LE: 2.75
	Mean (SD)	*RE: 2.03 (0.79); LE: 2.26 (0.61)*	*RE: 3.63 (0.55); LE: 4.18 (0.73)*	*RE: 4.54 (1.68); 4.33 (1.33)*

S: strabismic; A: anisometropic; C: control; AE: amblyopic eye; FE: fellow eye; RE: right eye; LE: left eye.

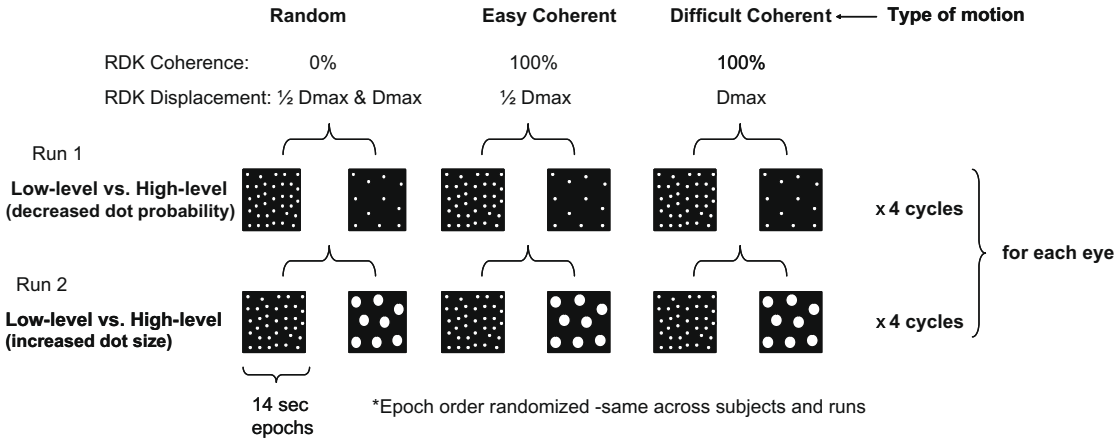

Fig. 1. Paradigm used for functional MRI scans. Each of the two Dmax runs had six epochs that were repeated for four cycles. The first run and the second run differed only in the high-level RDK stimulus used (reduced dot density or increased dot size). Both runs were based on the same block design and the order of the epochs was presented in the same predetermined, randomized order for each run and for every subject.

(6) 20 min dots at 0.5% density (Condition 2); Dmax; 100%.

The six epoch parameters for the second Dmax run were the same as above for epochs 1–3 but with the following changes for epochs 4–6:

(4) 1 deg dots at 5% density (Condition 3); Dmax or ½ Dmax (randomized); 0%.
(5) 1 deg dots at 5% density (Condition 3); ½ Dmax; 100%.
(6) 1 deg dots at 5% density (Condition 3); Dmax; 100%.

The order of the epochs was presented in the same predetermined randomized order for each run and for every subject. Participants had the task on all trials of pressing one of two buttons to indicate the perceived direction of the apparent motion (up or down) for each trial (even for the random motion trials in which neither was correct). For the four cycles, the order of the 6 epochs was: 1st cycle [6,1,5,4,2,3], 2nd cycle [5,1,3,2,4,6], 3rd cycle [6,4,2,3,1,5], 4th cycle [3,2,4,5,1,6]. The order of blocks was symmetrical (cycles 3 and 4 were the reverse of the order for cycles 1 and 2) to reduce the influence of linear trends. Every epoch contained 5 trials. Each trial was composed of 10 frames (the same number as in the psychophysical tasks) followed by an inter-trial interval of 800 ms during which a direction discrimination response was made. The random motion stimulus was created such that each frame was a new pattern of randomly placed dots and each dot traveled the same distance (either ½ Dmax or Dmax) between frames. Accuracy of behavioral responses was recorded for each of the coherent motion trials to confirm that level of difficulty and attention to the task were similar across subjects. Table 3 summarizes the accuracy scores for each participant.

Table 3
Individual subject accuracy scores obtained during fMRI scanning for amblyopic and fellow eyes.

Group	Subject	Ambylopic eye (%)	Fellow eye (%)
S	A	81	81
	B	78	74
	C	69	58
A	D	73	64
	E	69	70
	F	74	81
	G	73	51
	Mean (SD)	*74 (4)*	*68 (11)*
		Right eye (%)	Left eye (%)
C	H	62	75
	I	82	59
	J	88	86
	K	88	71
	Mean (SD)	*80 (12)*	*73 (11)*

S: strabismic; A: anisometropic; C: control.

3. Data analysis & results

Data preprocessing and statistical analysis were conducted with BrainVoyager QX (Brain Innovation). Prior to analysis, inter-slice time differences were removed from the data with an algorithm involving linear interpolation over time. All volumes were then corrected for small translational and rotational head movements by aligning to the first volume of each run using a nine-parameter rigid-body intensity-based algorithm with tri-linear interpolation across eight neighboring voxels. The motion correction values obtained from each group showed that motion during the course of the scans was within acceptable limits and similar across all subjects. The maximal translational and rotational motion correction values observed for each group were as follows: strabismic group = 0.60 mm and 0.68 deg; anisometropic group = 0.63 mm and 0.67 deg; control group = 0.49 mm and 0.45 deg. Temporal high-pass filtering (three cycles in time course) and a linear trend removal algorithm were used to eliminate temporal drifts from the data (e.g. physiological and scanner noise). The functional volumes were co-registered with the anatomic image. The data were then spatially normalized to stereotaxic space (Talairach & Tournoux, 1988) and superimposed onto the respective averaged anatomic images: strabismic, anisometropic, or control for the group analyses.

3.1. Whole brain voxelwise analysis

To identify the motion-sensitive areas showing differences in cortical activation for the low-level and high-level RDKs, analysis was done both for individual subjects, as well as for each of the three groups. Data for each eye were averaged together. The general linear model was used to analyze the data in a fixed-effects whole brain 3×2-factor ANOVA. A boxcar function, convolved with the BrainVoyager default haemodynamic response function (double-gamma function model; Friston et al., 1998) was used to model the data and maps of the t statistic were created, with a

Bonferroni correction for multiple comparisons ($p < 0.001$). The ANOVA was of the following factorial design:

Factor A *(three levels): type of Motion [Random, Easy coherent, Difficult coherent].*
Factor B *(two levels): type of RDK [Low-level, High-level].*

The first main effect tested looked at activation differences for direction discrimination of 100% coherent motion at ½ Dmax (easier task; Factor A2), coherent motion at Dmax (more difficult task; Factor A3) displacements relative to random motion (0% coherence) at random displacements (Factor A1). The second main effect, and that pertaining specifically to the test of our hypothesis, looked at activation differences between experimental (high-level; Conditions 2 or 3) versus the baseline (low-level; Condition 1) RDKs. For the ANOVA, the first predictor for each factor (Factor A: random motion; Factor B: low-level Condition 1) was excluded and used as the implicit baseline. Factor A × Factor B interactions were also tested.

In all three groups, there was no significant main effect of type of motion (Factor A: coherent motion (for easy or difficult direction discrimination) vs. random motion but there was a robust main effect of type of RDK (Factor B: high-level vs. low-level). There were no significant interactions.

Table 4 lists the brain areas showing significant cortical activation for this high-level vs. low-level comparison in the strabismic, anisometropic, and control groups. The number of individual subjects showing significant activation in the same brain regions is also presented. Although analysis was done on the whole brain, observed activation was limited to posterior brain regions. No significant activation was observed in anterior brain areas. Fig. 2 depicts the cortical activation observed for three subjects, one from each group (control, anisometropic, and strabismic). No smoothing algorithm was applied to define the areas and only cortical areas with greater than 50 contiguous voxels (BrainVoyager default cluster size limit) showing significant differences in activation for all high-level comparisons are listed in Table 4. The posterior occipital areas of activation were large in all three groups and included lower visual areas in both hemispheres. The MT + area was the cluster of contiguous activated voxels in the region of the parietal–temporal–occipital junction in each hemisphere. The stereotaxic locations of putative area V3A[2] (e.g. Dupont et al., 1994; Sunaert et al., 1999; Tootell et al., 1997) and MT+ (e.g. Sunaert et al., 1999; Tootell et al., 1995; Zeki et al., 1991) were consistent with locations reported in previous studies. Any parietal cortex activation observed was localized to the posterior-dorsal regions of the intraparietal sulcus (IPS) (Dupont et al., 1994; Orban et al., 2006; Sunaert et al., 1999).

Fig. 3 illustrates the general pattern of cortical activation observed in the control, anisometropic, and strabismic groups with a sample of coronal, and sagittal slices for the high-level vs. low-level comparison. The statistical maps are shown on the three group-averaged anatomic images. In support of our hypothesis, we observed a lesser response in cortical activation in posterior occipital regions and a greater response in activation in extra-striate motion areas in the control group when activation for high-level stimuli was compared to that for the low-level RDK. A similar pattern of activation differences was observed in the anisometropic group, although extent of activation appeared to be considerably smaller. In the strabismic group, there was relatively little difference in the cortical activation for high-level compared to the baseline with the exception of subtle activation in the posterior occipital area. With the conservative significance threshold selected (Bonferroni-corrected $p < 0.001$), there were no active voxels in areas corresponding to putative V3A and MT+, and very few (<50) contiguous, active voxels in PPC. This suggests that cortical activity in these areas is not significantly different for high-level and low-level RDKs.

3.2. Post-hoc region-of-interest analysis of percent blood oxygenation level dependent (BOLD) signal change

The reduced extent of cortical activation observed with anisometropic and strabismic amblyopia in the whole-brain analyses might be due to reduced gray matter volume. Using an automated computational method in the analysis of structural MRI images called voxel-based morphometry, Mendola and colleagues (2005) showed structural changes associated with amblyopia. They found reduced gray matter volume in the striate and extra-striate visual cortex of children with strabismic and anisometropic amblyopia. Alternatively, the group differences observed above could reflect lower signal strength in the amblyopic groups. ROI analysis of percent BOLD signal change allowed us to compare signal strength across the three groups.

The ROIs were selected from averaged data for both eyes of the control group and were defined as clusters of contiguous activated voxels centered at the peaks of activation obtained from the whole-brain analysis. The cursor was placed at the centre of activation and the BrainVoyager ROI analysis tool was used to demarcate the boundaries in both left and right hemispheres. We kept a conservative significance level ($p < 0.001$, Bonferroni-corrected) in order to keep the ROI distinct from other activation clusters. The boundary of the clusters was limited to a volume of 1000 mm^3 (spread range of 10 voxels in x, y, z directions in each hemisphere). The clusters from both hemispheres were then combined to create 4 ROIs: occipital, MT+, putative V3A, and parietal. No smoothing algorithm was applied to define the ROI. The small ROI size was chosen to minimize the number of non-active voxels within each ROI. The same 4 ROIs were kept consistent for analysis across the three groups.

Only comparisons of high-level vs. low-level RDKs were investigated post-hoc as this was the only statistically significant effect in the whole-brain ANOVA. A ROI GLM analysis was performed in each of the 4 ROIs for the control, strabismic, and anisometropic groups with subject-specific predictors in order to obtain percent BOLD signal change values for each participant. Fig. 4 shows the average percent signal change obtained within each of the motion-sensitive regions for the strabismic, anisometropic, and control groups (averaged across both eyes and both high-level conditions). The upper graph illustrates the greater percent BOLD signal response observed in extra-striate areas relative to that observed in the occipital areas for the comparison of high-level vs. low-level RDKs. Overall, percent BOLD signal was weaker for the strabismic than the control and anisometropic groups. Because ROI analysis has more statistical power than whole-brain analysis and because the ROIs were selected to be small so as to minimize noise from non-active voxels, the differences in activation between control and amblyopic groups are less than those determined using whole-brain statistics. The lower graph illustrates data for amblyopic and fellow eyes within each of the 4 ROIs (averaged across both amblyopic groups).

[2] This paper investigated general differences in patterns of neural activation for low-level (striate cortex) and high-level (extra-striate) motion processing in control and amblyopic children using first-order RDK stimuli that varied in dot size and dot density. Voxelwise analysis revealed statistically significant differences in cortical activation just inferior to the parieto-occipital sulcus in numerous subjects. These areas appeared to correspond to V3A based on previously reported stereotaxic coordinates. V3A is functionally defined and can only be accurately localized with retinotopic mapping (Tootell et al., 1997). Therefore, to make definitive conclusions regarding area V3A and further characterize activity in striate areas, retinotopic mapping would be necessary. Rather than omit these findings we chose to report on them and refer throughout the paper to the region as extra-striate area "putative V3A" to be proper.

Table 4
Results of whole brain voxelwise group analyses: significant cortical activation differences for high-level vs. baseline low-level RDK comparisons (significance level of $p < 0.001$ Bonferroni-corrected).

Group	Brain region (number of subjects/group with similar region)		Hemisphere	Extent (mm^3)	X	Y	Z	Average *t*-statistic	Statistical threshold
Strabismic	Occipital (2/3)		R/L	1148	9	−77	2	−6.50	$p < 10^{-9}$
	Putative V3A (1/3)			0[a]					
	MT+ (1/3)			0[a]					
	Parietal (2/3)	DIPSM	R	18[b]	22	−57	57	+5.70	$p < 10^{-8}$
Anisometropic	Occipital (4/4)		R/L	2869	−6	−69	−18	−7.88	$p < 10^{-10}$
	Putative V3A (2/4)		R	86	23	−71	18	+6.17	$p < 10^{-9}$
			L	63	−25	−68	26	+6.57	$p < 10^{-9}$
	MT+ (3/4)		L	80	−44	−63	15	+6.09	$p < 10^{-9}$
	Parietal (3/4)	POIPS	R	282	21	−56	36	+6.23	$p < 10^{-9}$
			L	759	−20	−57	41	+6.57	$p < 10^{-9}$
		VIPS	R	174	19	−64	40	+6.40	$p < 10^{-9}$
Control	Occipital (4/4)		R/L	34214	−1	−85	−11	−12.12	$p < 10^{-10}$
	Putative V3A (3/4)		R	2343	31	−79	16	+6.33	$p < 10^{-9}$
			L	1293	−23	−83	17	+6.24	$p < 10^{-9}$
	MT+ (3/4)		R	3800	40	−70	2	+6.62	$p < 10^{-9}$
			L	2634	−45	−76	1	+6.71	$p < 10^{-9}$
	Parietal (3/4)	DIPSM	R	992	22	−65	50	+6.53	$p < 10^{-9}$
			L	106	−16	−62	53	+5.96	$p < 10^{-9}$
		POIPS	R	109	32	−58	38	+5.99	$p < 10^{-9}$
			L	76	−20	−59	46	+5.89	$p < 10^{-9}$
		VIPS	R	2589	15	−78	38	+6.83	$p < 10^{-9}$
			L	103	−17	−78	46	+6.02	$p < 10^{-9}$
				174	−19	−82	33	+6.11	$p < 10^{-9}$

Talairach coordinate system for stereotaxic location: X: right–left; Y: anterior–posterior; Z: dorsal–ventral.
DIPSM: dorsal intraparietal sulcus medial; POIPS: parieto-occipital intraparietal sulcus; VIPS: ventral intraparietal sulcus
Regions listed above are for cluster sizes > 50 active voxels only (unless otherwise marked).
[a] No active voxels.
[b] No significant ROI cluster > 50 voxels.

To look further at the differences in signal strength between the three groups, a univariate ANOVA was conducted with the average percent BOLD signal change values obtained for every subject (in each eye, and for each region) as the dependent variable. Because we were interested in looking at the overall strength of cortical activation in either direction (positive or negative activation), the absolute value was used for any negative percent BOLD signal values. The percent BOLD signal change values used represented any differences in the cortical activity (motion processing) for high-level relative to the baseline low-level RDK.

Factors included in the analysis were: brain region (occipital, putative V3A, MT+, PPC); eye (fellow/right; amblyopic/left); group (strabismic, anisometropic, control); and high-level condition (increased dot size, decreased dot density). There were no significant interactions. Significant main effects of brain region ($F_{(3,56)} = 17.10$, $p = 0.00$), and group were obtained ($F_{(2,56)} = 3.01$, $p < 0.05$). There was no significant main effect of eye ($p = 0.41$) or high-level condition ($p = 0.24$). Interactions of group × eye ($p = 0.49$), group × region ($p = 0.80$) and region × eye ($p = 0.50$) were not significant. Bonferroni multiple comparisons showed that overall strength of cortical activation was greater in the occipital region ($M = 0.35\%$, $SD = 0.22\%$) than PPC ($M = 0.11\%$, $SD = 0.10\%$; $p = 0.00$), MT+ ($M = 0.09\%$, $SD = 0.06\%$; $p = 0.00$), or putative V3A ($M = 0.08\%$, $SD = 0.05\%$; $p = 0.00$) areas. Within the extra-striate regions, activation was similar between PPC, MT+, and putative V3A (all comparisons non-significant with $p = 1.00$). Strength of % BOLD signal was significantly less in the strabismic group ($M = 0.11\%$ $SD = 0.13\%$) than the control group ($M = 0.18\%$, $SD = 0.17\%$; $p < 0.05$) but not the anisometropic group ($M = 0.15\%$ $SD = 0.20\%$ $p < 0.23$). There was no significant difference in strength of percent BOLD signal change between anisometropic and control groups ($p = 0.68$). The results suggest that functional/signal strength deficits (in addition to structural/gray matter deficits) may account for differences in cortical activation observed between control and amblyopic groups in the whole-brain analyses, particularly for the strabismic group.

Correlations between stereoacuity, W4D score and percent signal change (absolute values) were tested. Neither stereoacuity ($r = -0.09$, $p = 0.58$) nor W4D scores ($r = 0.06$, $p = 0.73$) were significantly correlated to absolute percent BOLD signal values.

4. Discussion

Decreasing dot density and/or increasing dot size of first-order, luminance-defined RDKs create a bias towards high-level motion mechanisms (Sato, 1998; Smith & Ledgeway, 2001). In agreement with this, the whole-brain analysis result shows relatively less activation within lower-level areas (posterior occipital cortex) for high-level (decreased dot density or increased dot size) RDKs relative to the low-level baseline condition. This pattern of activation was observed in strabismic, anisometropic and control groups. For the same comparisons, we found greater activation in putative area V3A, area MT+, and posterior parietal regions of the IPS in the control group but to a lesser extent in the anisometropic and strabismic groups. The posterior IPS regions involved are consistent with those previously implicated in motion processing in humans (Claeys et al., 2003; Culham et al., 1998; Dupont et al., 1994; Sunaert et al., 1999). The strength of the percent BOLD signal change (positive or negative) relative to baseline was greatest in the anisometropic and control groups and less in the strabismic group even when Dmax was determined individually for each eye of each subject.

Numerous fMRI studies (Lerner et al., 2003; Lerner et al., 2006; Muckli et al., 2006) have shown reduced activation at higher-level areas of the ventral stream in amblyopic individuals. The general trend was for the extent of deficits to increase progressively from lower visual areas to higher visual areas. Extra-striate deficits were

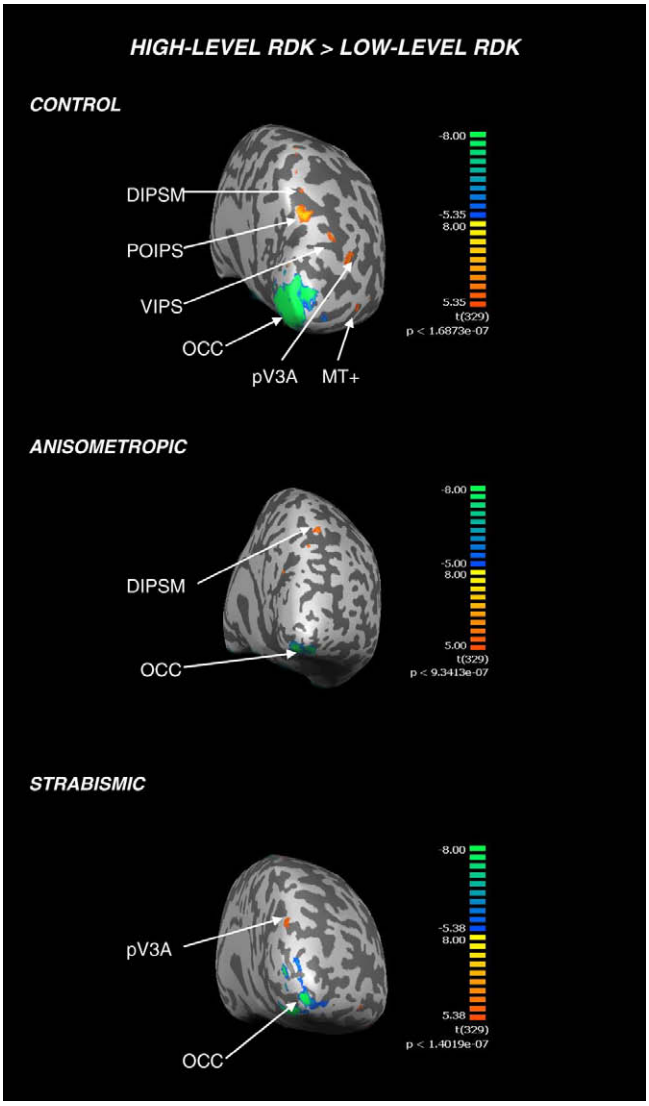

Fig. 2. Data for individual subjects from each group showing the significant activation obtained for comparisons of high-level vs. low-level RDKs on inflated cortical maps for the right hemisphere. The posterior view of the brain is presented because significant activation was observed only in this part of the brain. Significance level thresholds were matched as closely as possible across the three subjects to allow for comparison. Blue–green colors represent significant negative *t*-statistic values (lesser activation relative to baseline) and red–yellow colors represent significant positive *t*-statistic values (greater activation). The figures represent data from both eyes since there was no significant difference in cortical activation obtained for amblyopic vs. fellow eye viewing. *Top*: Activation for a control participant showing posterior occipital cortex, area MT+, putative V3A, and PPC activation. *Middle*: activation for an anisometropic participant. Pattern of activation is similar to the control subject but extent of activation is significantly less especially in the extra-striate regions. This subject had no significant activation in MT+ or putative V3A. *Bottom:* activation for a strabismic participant. There is primarily only posterior occipital cortex activity. (For interpretation of the references to color in this figure legend, the reader is referred to the web version of this article.)

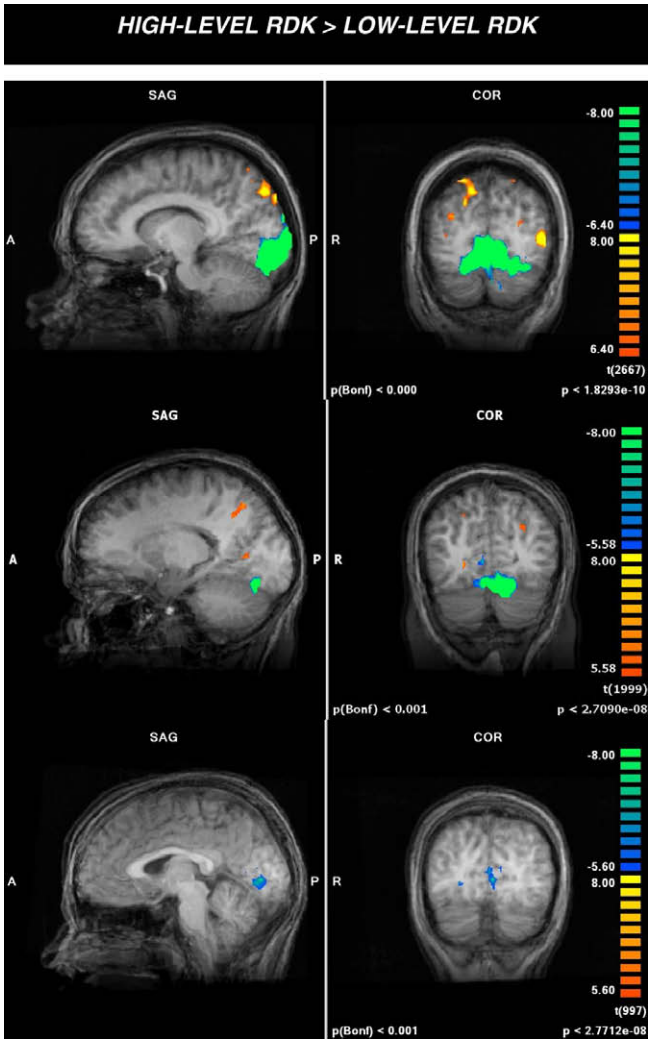

Fig. 3. Sample sagittal and coronal slices of images for brain areas identified in the voxelwise group analysis (at a significance level of $p < 0.001$ with a Bonferroni correction for multiple comparisons). Blue–green colors represent significant negative *t*-statistic values (lesser activation relative to baseline) and red–yellow colors represent significant positive *t*-statistic values (greater activation). The figures represent data from both eyes since there was no significant difference in cortical activation obtained for amblyopic vs. fellow eye viewing. *Top row images*: activation in the control group showing posterior occipital cortex, area MT+, putative V3A (inferior and posterior to activation in PPC), and PPC activation. *Middle row images*: activation in the anisometropic group. Pattern of activation is similar to controls but extent of activation is significantly less especially in the extra-striate regions. Area MT+ activation is not visible in these slices. *Bottom row images*: activation in the strabismic group. There is primarily only posterior occipital cortex activity. The extent of activation is significantly less for this group than for the anisometropic and control groups. (For interpretation of the references to color in this figure legend, the reader is referred to the web version of this article.)

most pronounced with amblyopic eye viewing and no significant difference was observed in the cortical activation pattern for anisometropic and strabismic amblyopia. The whole-brain analysis results from this study suggest that high-level areas of the dorsal stream appear to be impaired to a greater extent than low-level areas in amblyopia. However, there was no significant difference in cortical activation observed for amblyopic and fellow eyes. This is not surprising given that psychophysical Dmax thresholds are equally deficient in fellow and amblyopic eyes (Ho & Giaschi, 2006; Ho & Giaschi, 2007). Additional psychophysical evidence implicating high-level dorsal stream dysfunction in amblyopia includes deficits in attentive motion tracking (Ho et al., 2006), underestimation in visual object enumeration (Sharma, Levi, & Klein, 2000), and a prolonged attentional blink (Asper, Crewther, & Crewther, 2003), all of which involve PPC [(Culham et al., 1998 (attentive tracking), Sathian et al., 1999 (enumeration); Marios, Chun, & Gore, 2000 (attentional blink)].

4.1. Stimulus considerations

The differences in extent of activation and percent BOLD signal change are not likely accounted for by variability in task perfor-

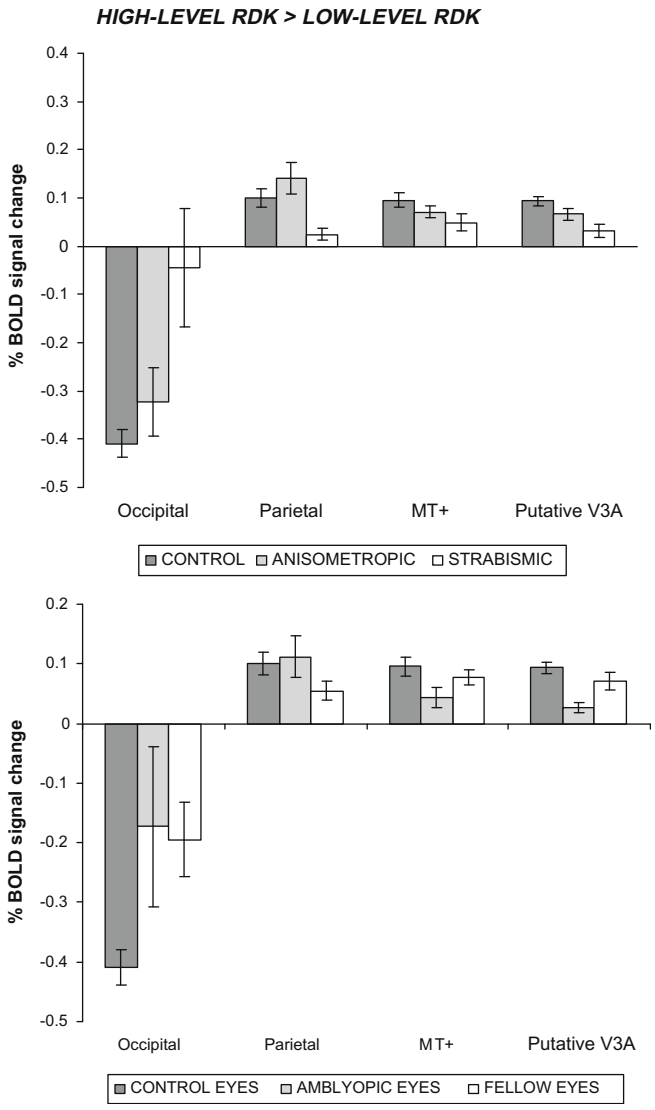

Fig. 4. Bar graph depicting percent BOLD signal change in the four brain regions for the comparison of high-level vs. low-level RDK stimuli. *Top:* the average percent signal change is plotted for each group: control, anisometropic and strabismic (averaged across both eyes). There was a statistically significant reduction in activation for high-level RDKs relative to the low-level baseline RDK in occipital cortex. In contrast, for the same comparison, there was a greater BOLD response in extra-striate motion areas. The strabismic group had significantly lower BOLD signal strength relative to anisometropic and control groups. *Bottom:* the average percent signal change is plotted for amblyopic and fellow eyes (averaged across both amblyopic groups). There was no significant difference in BOLD signal strength between fellow and amblyopic eyes.

mance across the groups. Behavioral responses were tracked and accuracy of direction discrimination (see Table 3) was not significantly greater for any one group. The fMRI stimuli used also considered the reduced visual acuity of the amblyopic participants. The stimuli were of high contrast (white dots on a black background). The central white fixation cross was large enough to be visible to even those participants with significantly reduced best-corrected visual acuity. The smallest dot size used was 20 min which is equivalent to the minimum angle of resolution of a 6/120 optotype (equal to decimal visual acuity of 0.05).

We can not rule out that the pattern of cortical activation observed may be related to the reduction in mean luminance or contrast with the less complex high-level stimuli relative to the low-level stimuli. Although this might account for some of the reduced activity in low-level occipital areas, it is not likely to explain all of the findings reported. Firstly, if Dmax was mediated through a mechanism dependent only on contrast, decreasing dot probability (for example) would result in a decrease in Dmax, which is inconsistent with psychophysical findings of an increase in Dmax. Secondly, if extra-striate areas were influenced primarily by luminance or contrast, a stronger BOLD response might be expected with an increase, not a decrease, in stimulus luminance or contrast (Logothetis, Pauls, Augath, Trinath, & Oeltermann, 2001). We report a greater response in PPC despite the decrease in mean luminance that accompanies the less complex, high-level RDK stimuli. Other studies have reported that BOLD fMRI responses in extra-striate visual areas are invariant to changes in luminance contrast (Goodyear & Menon, 1998) with respect to spatial extent of activation as well as to percent change in signal intensity. Thus, mechanisms other than (or in addition to) those which are luminance-dependent are likely involved in explaining the pattern of cortical activity observed in extra-striate cortex.

4.2. The role of eye movements

Bedell and Flom (1985) reported bilateral oculomotor abnormalities in strabismic individuals with amblyopia. While it is possible that abnormal eye movements and fixation in fellow eyes could contribute to the different results for the strabismic group, this seems unlikely to be the case. Firstly, none of our subjects had eccentric fixation. Secondly, to minimize the influence of horizontal eye movements (nasal drifts or asymmetric pursuits) in the direction discrimination task, RDK motion was deliberately chosen to be in a vertical direction. As dot displacement approaches Dmax, stimulus speed/velocity also increases, and the task becomes more difficult. Theoretically, children would perceive direction of motion as oblique rather than vertical for larger dot displacements (Souman, Hooge, & Wertheim, 2005) due to interference from horizontal eye movements. This would make the task of vertical direction discrimination more difficult and performance would be expected to be worse. However, this is not the case with this sample of strabismic subjects. In fact, Dmax was occasionally greater than that obtained in control and anisometropic participants (Table 2).

4.3. Relationship to binocularity

McKee and colleagues (McKee, Levi, & Movshon, 2003) found level of residual binocularity to be a better indicator of psychophysical performance than the type of amblyopia. Using RDK stimuli similar to that used in this study, amblyopic children with poor stereoacuity tended to have increased Dmax relative to those with normal stereoacuity (Ho & Giaschi, 2007). This was true for anisometropic and strabismic amblyopia. That study found the strength of correlation was greatest within the strabismic group and most noticeable for RDKs biasing the high-level motion system for both groups. Although amblyopic children demonstrate psychophysical deficits in both low-level and high-level motion mechanisms compared to control children, the high-level, feature-matching mechanism may be relatively spared when fine stereopsis is absent (Ho & Giaschi, 2007). Dmax for direction discrimination and Dmax for disparity detection are similar in value (Glennerster, 1998) suggesting some overlap between correspondence mechanisms for motion and depth perception. Others (McColl, Ziegler, & Hess, 2000; Wilcox & Hess, 1995) have reported on the persistence of a coarser-scaled, non-linear stereopsis mechanism despite deficits in finer-scaled, linear stereopsis mechanisms. McColl and colleagues suggested that the coarser-scaled disparity mechanism may benefit correspondence mechanisms by possibly reducing the probability of false-matches, improving detection of object features as well as minimizing diplopia.

In this study, poor binocular function was not significantly correlated with reduced strength of BOLD signal. The strabismic group was also the group with the poorest binocularity. The lack of cortical activation differences between high- and low-level RDKs, particularly in extra-striate areas, could be possible if both types of RDK stimuli were processed by a common mechanism. If this group has sparing of high-level, coarse-scaled correspondence mechanisms, then strabismic children may use high-level correspondence mechanisms for both high-level and low-level RDK stimuli. The lack of cortical activation might represent a deficit in low-level rather than high-level mechanisms for this group.

4.4. General conclusions

We observed less activation in extra-striate motion-sensitive areas of anisometropic and strabismic groups relative to controls. The extra-striate deficits appeared larger for the strabismic group than the anisometropic group when activation for high-level RDK stimuli were compared to the baseline low-level RDK. The percent BOLD signal strength was also less in the strabismic group than the anisometropic and control groups. One hypothesis explaining the group differences is that high-level motion processing mechanisms may be deficient especially in strabismic amblyopia. This might be attributed to decreased gray matter in amblyopia (Mendola et al., 2005) or to reduced/altered neural activity in these brain regions. The extent or strength of neural input into a specific brain area has been reported to be closely associated with the BOLD response observed in that region (Logothetis, 2002; Logothetis et al., 2001). Neural deficits in strabismic amblyopia have been associated with decreased synchronization of neurons (Roelfsema, Konig, Engel, Sireteanu, & Singer, 1994) which impair the strength of neural input into higher-level areas (Anderson, Holliday, & Harding, 1999; Anderson & Swettenham, 2006). Thus deficits in extra-striate cortex function may be explained by a progressive degradation of feed-forward neural signals in the dorsal pathway such that input to target high-level motion-sensitive cortex is weakened. Consequent impaired feedback from extra-striate cortex may then be partly responsible for reduced activation in lower-level areas as seen in the occipital cortex of the amblyopic groups. For example, V1 activity has been found to be mediated by feedback from MT+ in the perception of long-range (high-level) apparent motion (Sterzer, Haynes, & Rees, 2006).

However, there is behavioral evidence supporting a relative sparing of high-level, coarse-scale correspondence mechanisms (Ho & Giaschi, 2007; McColl et al., 2000; Wilcox & Hess, 1995) in strabismic (non-binocular) amblyopia despite poor stereoacuity. Therefore, an alternative hypothesis explaining the extra-striate deficits in the non-binocular (strabismic) group for high-level vs. low-level comparisons, is a predominance of high-level, feature-matching mechanisms (over low-level mechanisms) in motion processing for *both* low-level and high-level RDK stimuli. Future studies will explore these two contradictory theories with larger sample sizes so that cortical activation patterns observed in this study can be confirmed through random effects analysis. Given the robust cortical differences observed in occipital cortex for both control and amblyopic groups when comparing activation for low-level and high-level, first-order RDKs, future studies will also focus on delineating and characterizing the activity and deficits in retinotopic visual areas.

Acknowledgments

This research was supported by NSERC Grant 194526 to D. Giaschi. C. Ho received funding from the Canadian Optometric Education Trust Fund (Canadian Association of Optometrists), the BC Research Institute in Children's and Women's Health, and the BC Ministry of Children & Family Development through the Human Early Learning Partnership. The authors wish to thank B. Lee for computer programming; B. Maedler and Philips Medical Systems; T. Harris, P. Coutts, R. Cheema, C. Boden for assistance with data collection at the University of British Columbia MRI Research Centre; S. Au Young, K. Fitzpatrick for help with data analysis at the Children's Brain Mapping Centre, BC's Children's Hospital.

References

Anderson, S. J., Holliday, I. E., & Harding, G. F. A. (1999). Assessment of cortical dysfunction in human strabismic amblyopia using magnetoencephalography (MEG). *Vision Research, 39*, 1723–1738.

Anderson, S. J., & Swettenham, J. B. (2006). Neuroimaging in human amblyopia. *Strabismus, 14*, 21–35.

Asper, L., Crewther, D., & Crewther, S. (2000). Strabismic amblyopia – Part 1: Psychophysics. *Clinical and Experimental Optometry, 83*, 49–58.

Asper, L., Crewther, D., & Crewther, S. (2003). Do different amblyopes have different attentional blinks? *Investigative Ophthalmology & VisualScience*, S4094.

Barnes, G. R., Hess, R. F., Dumoulin, S. O., Achtman, R. L., & Pike, G. B. (2001). The cortical deficit in humans with strabismic amblyopia. *Journal of Physiology, 15*, 281–297.

Battelli, L., Cavanagh, P., Intriligator, J., Tramo, M. J., Henaff, M. A., Michel, F., et al. (2001). Unilateral right parietal damage leads to bilateral deficit for high-level motion. *Neuron, 32*, 985–995.

Bedell, H. E., & Flom, M. C. (1985). Bilateral oculomotor abnormalities in strabismic amblyopes: Evidence for a common central mechanism. *Documenta Ophthalmologica, 59*, 309–321.

Birch, E. E., & Swanson, W. H. (2000). Hyperacuity deficits in anisometropic and strabismic amblyopes with known ages of onset. *Vision Research, 40*, 1035–1040.

Braddick, O. (1974). A short-range process in apparent motion. *Vision Research, 14*, 519–527.

Buckingham, T., Watkins, R., Bansal, P., & Bamford, K. (1991). Hyperacuity thresholds for oscillatory movement are abnormal in strabismic and anisometropic amblyopes. *Optometry and Vision Science, 68*, 351–356.

Cavanagh, P. (1992). Attention-based motion perception. *Science, 257*, 1563–1565.

Cavanagh, P., & Mather, G. (1990). Motion: The long and short of it. *Spatial Vision, 4*, 103–129.

Cheng, K., Fujita, H., Kanno, I., Miura, S., & Tanaka, K. J. (1995). Human cortical regions activated by wide-field visual motion: An H_2O PET study. *Journal of Neurophysiology, 74*, 413–427.

Claeys, K. G., Lindsey, D. T., De Schutter, E., & Orban, G. A. (2003). A higher order motion region in human inferior parietal lobule: Evidence from fMRI. *Neuron, 40*, 631–642.

Culham, J. C., Brandt, S. A., Cavanagh, P., Kanwisher, N. G., Dale, A. M., & Tootell, R. B. (1998). Cortical fMRI activation produced by attentive tracking of moving targets. *Journal of Neurophysiology, 80*, 2657–2670.

Demanins, R., Wang, Y. Z., & Hess, R. F. (1999). The neural deficit in strabismic amblyopia: Sampling considerations. *Vision Research, 39*, 3575–3585.

Dumoulin, S. O., Baker, C. L., Jr., Hess, R. F., & Evans, A. C. (2003). Cortical specialization for processing first- and second-order motion. *Cerebral Cortex, 13*, 1375–1385.

Dupont, P., Orban, G. A., De Bruyn, B., Verbruggen, A., & Mortelmans, L. (1994). Many areas in the human brain respond to visual motion. *Journal of Neurophysiology, 72*, 1420–1424.

Dupont, P., Sary, G., Peuskens, H., & Orban, G. A. (2003). Cerebral regions processing first- and higher-order motion in an opposed-direction discrimination task. *European Journal of Neuroscience, 17*, 1509–1517.

Ellemberg, D., Lewis, T. L., Maurer, D., Brar, S., & Brent, H. P. (2002). Better perception of global motion after monocular than after binocular deprivation. *Vision Research, 42*, 169–179.

Friston, K. J., Fletcher, P., Josephs, O., Holmes, A., Rugg, M. D., & Turner, R. (1998). Event-related fMRI: Characterizing differential responses. *Neuroimage, 7*, 30–40.

Giaschi, D. E., Regan, D., Kraft, S. P., & Hong, X. H. (1992). Defective processing of motion-defined form in the fellow eye of patients with unilateral amblyopia. *Investigative Ophthalmology & Visual Science, 33*, 2483–2489.

Glennerster, A. (1998). Dmax for stereopsis and motion in random dot displays. *Vision Research, 38*, 925–935.

Goodyear, B. G., & Menon, R. S. (1998). Effect of luminance contrast on BOLD fMRI response in human primary visual areas. *Journal of Neurophysiology, 79*, 2204–2207.

Hess, R. F., Demanins, R., & Bex, P. J. (1997). A reduced motion aftereffect in strabismic amblyopia. *Vision Research, 37*, 1303–1311.

Ho, C. S., & Giaschi, D. E. (2006). Deficient maximum motion displacement in amblyopia. *Vision Research, 46*, 4595–4603.

Ho, C. S., & Giaschi, D. E. (2007). Stereopsis-dependent deficits in maximum motion displacement. *Vision Research, 47*, 2778–2785.

Ho, C. S., Giaschi, D. E., Boden, C., Dougherty, R., Cline, R., & Lyons, C. (2005). Deficient motion perception in the fellow eye of amblyopic children. *Vision Research, 45*, 1615–1627.

Ho, C. S., Paul, P. S., Asirvatham, A., Cavangh, P., Cline, R., & Giaschi, D. (2006). Abnormal spatial selection and tracking in children with amblyopia. *Vision Research, 46*, 3274–3283.

Jose, R. T., & Atcherson, R. M. (1977). Type-size variability for near-point acuity tests. *American Journal of Optometry and Physiological Optics, 54*, 634–638.
Kelly, S. L., & Buckingham, T. J. (1998). Movement hyperacuity in childhood amblyopia. *British Journal of Ophthalmology, 82*, 991–995.
Lerner, Y., Hendler, T., Malach, R., Harel, M., Leiba, H., Stolovitch, C., et al. (2006). Selective fovea-related deprived activation in retinotopic and high-order visual cortex of human amblyopes. *Neuroimage, 33*, 169–179.
Lerner, Y., Pianka, P., Azmon, B., Leiba, H., Stolovitch, C., Loewenstein, A., et al. (2003). Area-specific amblyopic effects in human occipitotemporal object representations. *Neuron, 40*, 1023–1029.
Levi, D. M. (1991). Spatial vision in amblyopia. In D. Regan (Ed.), *Spatial vision* (pp. 212–238). London: MacMillan.
Logothetis, N. K. (2002). The neural basis of the blood-oxygen-level-dependent functional magnetic resonance imaging signal. *Philosophical transactions of the Royal Society of London, Series B, 357*, 1003–1037.
Logothetis, N. K., Pauls, J., Augath, M., Trinath, T., & Oeltermann, A. (2001). Neurophysiological investigation of the basis of the fMRI signal. *Nature, 412*, 150–157.
Lu, Z.-L., & Sperling, G. (2001). Three-systems theory of human visual motion perception: Review and update. *Journal of the Optical Society of America Series A, 18*, 2331–2370.
Mansouri, B., Allen, H. A., & Hess, R. F. (2005). Detection, discrimination and integration of second-order orientation information in strabismic and anisometropic amblyopia. *Vision Research, 45*, 2449–2460.
Marios, R., Chun, M., & Gore, J. (2000). Neural correlates of the attentional blink. *Neuron, 28*, 299–308.
McColl, S. L., Ziegler, L., & Hess, R. F. (2000). Stereodeficient subjects demonstrate non-linear stereopsis. *Vision Research, 40*, 1167–1177.
McKee, S., Levi, D., & Movshon, A. (2003). The pattern of visual deficits in amblyopia. *Journal of Vision, 3*, 380–405.
Mendola, J. D., Conner, I. P., Roy, A., Chan, S. T., Schwartz, T. L., Odom, J. V., et al. (2005). Voxel-based analysis of MRI detects abnormal visual cortex in children and adults with amblyopia. *Human Brain Mapping, 25*, 222–236.
Milner, A. D., & Goodale, M. A. (1995). *The visual brain in action*. Oxford: Oxford University Press.
Muckli, L., Kiess, S., Tonhausen, N., Singer, W., Goebel, R., & Sireteanu, R. (2006). Cerebral correlates of impaired grating perception in individual psychophysically assessed human amblyopes. *Vision Research, 46*, 506–526.
Mussap, A. J., & Levi, D. M. (1999). Orientation-based texture segmentation in strabismic amblyopia. *Vision Research, 39*, 411–418.
Nishida, S., Sasaki, Y., Murakami, I., Watanabe, T., & Tootell, R. B. (2003). Neuroimaging of direction-selective mechanisms for second-order motion. *Journal of Neurophysiology, 90*, 3242–3254.
Nishida, S., & Sato, T. (1995). Motion aftereffect with flickering test patterns reveals higher stages of motion processing. *Vision Research, 35*, 477–490.
Orban, G. A., Claeys, K., Nelissen, K., Smans, R., Sunaert, S., Todd, J. T., et al. (2006). Mapping the parietal cortex of human and non-human primates. *Neuropsychologia, 44*, 2647–2667.
Parrish, E. E., Giaschi, D. E., Boden, C., & Dougherty, R. (2005). The maturation of form and motion perception in school age children. *Vision Research, 45*, 827–837.
Roelfsema, P. R., Konig, P., Engel, A. K., Sireteanu, R., & Singer, W. (1994). Reduced synchronization in the visual cortex of cats with strabismic amblyopia. *European Journal of Neuroscience, 6*, 1645–1655.
Rutstein, R. P., & Daum, K. M. (1998). Suppression and anomalous correspondence. In *Anomalies of binocular vision: Diagnosis & management* (pp. 116–118). St. Louis, Missouri: Mosby-Year Book, Inc.
Sathian, K., Simon, T. J., Peterson, S., Patel, G. A., Hoffman, J. M., & Grafton, S. T. (1999). Neural evidence linking visual object enumeration and attention. *Journal of Cognitive Neuroscience, 11*, 36–51.
Sato, T. (1998). Dmax: Relations to low- and high-level motion processes. In T. Watanabe (Ed.), *High-level motion processing, computational, neurobiological, and psychophysical perspectives* (pp. 115–151). Boston: MIT Press.
Schor, C. M., & Levi, D. M. (1980a). Disturbances of small-field horizontal and vertical optokinetic nystagmus in amblyopia. *Investigative Ophthalmology & Visual Science, 6*, 668–683.
Schor, C. M., & Levi, D. M. (1980b). Direction selectivity for perceived motion in strabismic and anisometropic amblyopia. *Investigative Ophthalmology & Visual Science, 9*, 1094–1104.
Seiffert, A. E., Somers, D. C., Dale, A. M., & Tootell, R. B. (2003). Functional MRI studies of human visual motion perception: Texture, luminance, attention and after-effects. *Cerebral Cortex, 13*, 340–349.
Sharma, V., Levi, D. M., & Klein, S. A. (2000). Undercounting features and missing features: Evidence for a high-level deficit in strabismic amblyopia. *Nature Neuroscience, 3*, 496–501.
Simmers, A. J., Ledgeway & Hess, R. F. (2005). The influences of visibility and anomalous integration processes on the perception of global spatial form versus motion in human amblyopia. *Vision Research, 45*, 449–460.
Simmers, A. J., Ledgeway, T., Hess, R. F., & McGraw, P. V. (2003). Deficits to global motion processing in human amblyopia. *Vision Research, 43*, 729–738.
Simmers, A. J., Ledgeway, T., Mansouri, B., Hutchinson, C. V., & Hess, R. F. (2006). The extent of dorsal extra-striate deficit in amblyopia. *Vision Research, 46*, 2571–2580.
Smith, A. T., Greenlee, M. W., Singh, K. D., Kraemer, F. M., & Hennig, J. (1998). The processing of first- and second-order motion in human visual cortex assessed by functional magnetic resonance imaging (fMRI). *Journal of Neuroscience, 18*, 3816–3830.
Smith, A. T., & Ledgeway, T. (2001). Motion detection in human vision: A unifying approach based on energy and features. *Proceedings of the Royal Society of London, Series B, Biological Sciences, 268*, 1889–1899.
Snowden, R. J., & Braddick, O. J. (1990). Differences in the processing of short-range apparent motion at small and large displacements. *Vision Research, 30*, 1211–1222.
Souman, J. L., Hooge, I. T., & Wertheim, A. H. (2005). Vertical object motion during horizontal ocular pursuit: Compensation for eye movements increases with presentation duration. *Vision Research, 45*, 845–853.
Steinman, S. B., Levi, D. M., & McKee, S. P. (1988). Discrimination of time and velocity in the amblyopic visual system. *Clinical Vision Science, 2*, 265–276.
Sterzer, P., Haynes, J. D., & Rees, G. (2006). Primary visual cortex activation on the path of apparent motion is mediated by feedback from hMT+/V5. *Neuroimage, 32*, 1308–1316.
Sunaert, S., Van Hecke, P., Marchal, G., & Orban, G. A. (1999). Motion-responsive regions of the human brain. *Experimental Brain Research, 127*, 355–370.
Talairach, J., & Tournoux, P. (1988). *Coplanar stereotaxic atlas of the human brain*. New York: Thieme.
Tootell, R. B., Mendola, J. D., Hadjikhani, N. K., Ledden, P. J., Liu, A. K., Reppas, J. B., et al. (1997). Functional analysis of V3A and related areas in human visual cortex. *Journal of Neuroscience, 17*, 7060–7078.
Tootell, R. B. H., Reppas, J. B., Kwong, K. K., Malach, R., Born, R. T., Brady, T. J., et al. (1995). Functional analysis of human MT and related visual cortical areas using magnetic resonance imaging. *Journal of Neuroscience, 15*, 3215–3230.
Ungerleider, L. G., & Mishkin, M. (1982). Two cortical visual systems. In D. J. Ingle, M. A. Goodale, & R. J. W. Mansfield (Eds.), *Analysis of visual behavior* (pp. 549–586). Cambridge: MIT Press.
Wichmann, F. A., & Hill, N. J. (2001). The psychometric function: I. Fitting, sampling, and goodness-of-fit. *Perception and Psychophysics, 63*, 1293–1313.
Wilcox, L. M., & Hess, R. F. (1995). Dmax for stereopsis depends on size, not spatial frequency content. *Vision Research, 36*, 391–399.
Zeki, S., Watson, J. D., Lueck, C., Friston, K. J., Kennard, C., & Frackowiak, R. S. J. (1991). A direct demonstration of functional specialization in the human visual cortex. *Journal of Neuroscience, 11*, 641–649.